

# When are selector control strategies optimal for constrained monotone systems? <sup>★</sup>

Hamed Taghavian <sup>a</sup>, Ross Drummond <sup>b</sup>, Mikael Johansson <sup>a</sup>

<sup>a</sup>*KTH Royal Institute of Technology, Stockholm, Sweden*

<sup>b</sup>*University of Sheffield, Sheffield, UK*

---

## Abstract

This paper considers optimal control problems defined by a monotone dynamical system, a monotone cost, and monotone constraints. We identify families of such problems for which the optimal solution is bang-ride, i.e., always operates on the constraint boundaries, and prove that the optimal policy switches between a finite number of state feedback controllers. This motivates the use of simpler policies, such as selector control, that can be designed without perfect models and full state measurements. The approach is successfully applied to several variations of the health-aware fast charging problem for lithium-ion batteries.

*Key words:* Optimal control; Monotone systems; Selector control; Fast charging; Lithium-ion battery; PID.

---

## 1 INTRODUCTION

Optimal control theory is a powerful framework for identifying the limits of performance of dynamical systems and for characterizing the controllers that operate at these limits. However, although several techniques exist for computing optimal open-loop trajectories, it is generally difficult to find optimal *feedback policies*. It has become increasingly popular to attempt to mimic optimal control policies using model-predictive controllers, but these are complex, memory-intensive, and require precise system models as well as significant online computations. For this reason, classical control designs remain highly popular in practice. In fact, it has been estimated that as much as 95% of controllers deployed in the industry are PIDs [17]. Easy implementation and commissioning, simple tuning and analysis, and low requirements on the controller hardware are some of the advantages that allow classical controllers to remain competitive with more advanced options.

When classical controllers are used to control complex systems, they are often combined with other simple com-

ponents to deliver the required flexibility and performance [3]. One such component is the min/max selector which is a nonlinear static device with multiple inputs and a single output. The selector uses simple logic to select one of the inputs, typically the one with the smallest or the largest value, and connect it to the output. Hence, a selector essentially isolates individual control loops during operation, allowing for single-loop design methods to be applied in more complex control settings, thus simplifying the overall design. We call a control system comprising a selector and multiple linear control loops a *selector control* system. Selector control systems are especially common in industrial applications where, for safety reasons, some variables must remain within certain limits, such as the grid frequency observed in power systems [3] and the chemical concentrations in process control [11]. Another application is found in engine control systems, where selectors are used in the feedback module to provide the desired thrust [21].

Compared with more advanced methods, such as model predictive control, selector control strategies are easier to implement and cheaper to execute. In addition, the individual control loops can often be tuned in a model-free fashion based on data. Despite these advantages, selector control is still applied in an ad-hoc manner and little is known about what problems it is expected to perform well on [11]. Identifying problems for which selector control strategies are optimal will justify their use

---

<sup>★</sup> This work was supported by KTH Royal Institute of Technology.

*Email addresses:* hamedta@kth.se (Hamed Taghavian), ross.drummond@sheffield.ac.uk (Ross Drummond), mikaelj@kth.se (Mikael Johansson).

in practice and could help to improve their tuning.

In this paper, it is shown that selector control policies are optimal for a class of monotone control problems. These problems aim at optimizing a monotone cost function subject to a monotone dynamical system with monotone constraints. We study the solutions to these problems using ideas from the calculus of variations and show how the inequality constraints become active during the optimal operation. The implication of this result is that the optimal solutions to certain monotone control problems can be implemented using selector control on industrially relevant hardware. While monotone control problems may seem restrictive at first, they find many practical applications in diverse areas such as molecular biology [2], transportation networks [19, 16], fast charging of batteries [6] and robotics [18]. Still, none of these papers prove and exploit the optimality of selector control.

This paper is organized as follows: We introduce the family of monotone optimal control problems in Section 2 and discuss their solutions in Section 3. A practical application of the results is provided in Section 4 and concluding remarks are given in Section 5.

### 1.1 Notation

The  $i^{\text{th}}$  entry of the element  $x_t \in \mathbb{R}^n$  in the sequence  $x = \{x_t\}_{t=0}^{t=t_f}$  is denoted by  $x_{i,t}$ . All inequalities are understood componentwise, *i.e.* for two  $n$ -vectors  $x_1$  and  $x_2$ ,  $x_1 \geq x_2$  means that  $x_{i,1} \geq x_{i,2}$  for all  $i = 1, 2, \dots, n$ .

## 2 MONOTONE OPTIMAL CONTROL

Consider the following discrete-time, possibly nonlinear, dynamical system with one input and multiple outputs

$$\begin{aligned} x_{t+1} &= f(x_t, u_t) \\ y_t &= h(x_t, u_t) \end{aligned} \quad \text{for } t \in \mathbb{N}_0. \quad (1)$$

Here,  $x_t \in \mathbb{R}^n$  is the state,  $y_t \in \mathbb{R}^p$  is the output vector and  $u_t \in \mathbb{R}$  is the input. For a given initial state  $x_0 \in \mathbb{R}^n$ , we study optimal control problems on the form

$$\begin{aligned} &\underset{u}{\text{maximize}} \quad J(x_0, u) = \sum_{t=0}^{t_f} L(x_t, u_t) \\ &\text{subject to} \quad y_t \leq y_{\max}, \\ &\quad \quad \quad u_t \leq u_{\max}, \\ &\quad \quad \quad u, x, y \text{ satisfy (1),} \end{aligned} \quad (2)$$

for constant  $u_{\max} \in \mathbb{R}$  and  $y_{\max} \in \mathbb{R}^p$ . For ease of notation, we have introduced  $u = \{u_t\}_{t=0}^{t=t_f}$ ,  $x = \{x_t\}_{t=0}^{t=t_f}$ , and  $y = \{y_t\}_{t=0}^{t=t_f}$ . Our results are derived under monotonicity assumptions on the functions  $f$ ,  $h$ , and  $L$ . To

describe these, we introduce the  $k$ -step reachable set of (1) from initial state  $z$  under the constraints of (2)

$$\mathcal{R}(z, k) = \{x_k \in \mathbb{R}^n \mid x_0 = z \text{ and } x_t, u_t, y_t \text{ satisfy (1)-(2) for all } t \in [0, k]\}$$

and let

$$\bar{\mathcal{R}}(x_0, t_f) = \bigcup_{k=0}^{t_f} \mathcal{R}(x_0, k)$$

In this way,  $\bar{\mathcal{R}}(x_0, t_f)$  represents the set of states that can be visited on the time interval  $[0, t_f]$  from initial state  $x_0$  under the dynamics (1) while satisfying the constraints of (2). We also need the following definition.

**Definition 1.** Let  $\mathcal{D}_x \subseteq \mathbb{R}^n$  and  $\mathcal{D}_u \subseteq \mathbb{R}$ . A function  $g : \mathbb{R}^n \times \mathbb{R} \rightarrow \mathbb{R}^{n_g}$  is increasing in  $\mathcal{D}_x \times \mathcal{D}_u$  if for all  $x_1, x_2 \in \mathcal{D}_x$  and  $u_1, u_2 \in \mathcal{D}_u$  we have

$$x_1 \geq x_2 \text{ and } u_1 \geq u_2 \Rightarrow g(x_1, u_1) \geq g(x_2, u_2)$$

Hence, a function  $g$  is increasing if and only if all its components  $g_1, \dots, g_{n_g}$  are increasing.

We make the following sequence of assumptions.

**Assumption 1** (monotone cost). *The running cost  $L(x_t, u_t)$  is continuous and increasing in  $(x_t, u_t) \in \mathbb{R}^n \times \mathbb{R}$ .*

**Assumption 2** (monotone system). *The transition function  $f(x_t, u_t)$  is continuous in  $(x_t, u_t) \in \mathbb{R}^n \times \mathbb{R}$  and is increasing in the region  $(x_t, u_t) \in \bar{\mathcal{R}}(x_0, t_f) \times (-\infty, u_{\max}]$ .*

**Assumption 3** (monotone constraint). *The output function  $h(x_t, u_t)$  is continuous in  $x_t \in \mathbb{R}^n$  for all  $u_t \in (-\infty, u_{\max}]$ , and both differentiable and strictly increasing in  $u_t \in \mathbb{R}$  for all  $x_t \in \bar{\mathcal{R}}(x_0, t_f)$ .*

Under Assumption 2, the dynamical system (1) is a monotone control system in the sense of [2], because

$$\hat{x}_0 \geq x_0 \text{ and } \hat{u}_t \geq u_t \forall t \in \mathbb{N}_0 \Rightarrow \hat{x}_t \geq x_t \forall t \in \mathbb{N}_0$$

which is readily shown by induction. When  $f$  is differentiable, Assumption 2 states that

$$\partial f_i(x_t, u_t) / \partial u_t \geq 0, \quad \partial f_i(x_t, u_t) / \partial x_{j,t} \geq 0 \quad (3)$$

holds everywhere in  $(x_t, u_t) \in \bar{\mathcal{R}}(x_0, t_f) \times (-\infty, u_{\max}]$  for all  $i, j \in \{1, 2, \dots, n\}$ .

Assumption 3 states that

$$\partial h_i(x_t, u_t) / \partial u_t \geq 0, \quad i = 1, 2, \dots, p$$

holds for all  $x_t \in \bar{\mathcal{R}}(x_0, t_f)$  and  $u_t \in \mathbb{R}$ , with equality met only on a set of zero measure. Therefore, since

$\partial h_i(x_t, u_t)/\partial u_t \neq 0$  holds almost everywhere,

$$h(x_t, \hat{u}_t) > h(x_t, u_t) \quad (4)$$

is satisfied whenever  $\hat{u}_t > u_t$ . Assumption 3 is less restrictive than it seems because the inequality constraints associated with the output functions that are decreasing in  $u_t$  can be safely removed from the optimization problem (2) with no impact on the optimal value. To see why, we first note that by combining Assumptions 1 and 2 one can show that  $L(x_t, u_t)$  is increasing in  $u_k$  for all  $k \in \{0, 1, \dots, t\}$ , and therefore, the cost function in (2) is also increasing in  $u_t$ . Hence, there are optimal solutions to (2) in which the inequality constraints associated with the output functions that are decreasing in  $u_t$  are not activated (except in degenerate cases where those constraints are explicitly enforced for all feasible  $x$ , e.g. the equality constraint  $u_t = 1$  enforced by the double inequality  $h(x_t, u_t) = \begin{bmatrix} -u_t & u_t \end{bmatrix}^T \leq y_{\max} = \begin{bmatrix} -1 & 1 \end{bmatrix}^T$ ).

When the output map does not depend on  $u_t$ , *i.e.* when  $h_i(x_t, u_t) = h_i(x_t)$ , Assumption 3 is not satisfied. However, one may then redefine the  $i$ -th output to be

$$\hat{h}_i(x_t, u_t) = h_i \circ f_a^d \circ f(x_t, u_t) \quad (5)$$

where  $f_a(\cdot) = f(\cdot, 0)$  is the autonomous system dynamics in (1),  $f_a^d$  is the  $d$ -fold composition of  $f_a$  with itself and  $d \in [0, n-1] \cup \{\infty\}$  is the relative degree of the  $i$ -th output in the nonlinear dynamic system (1). Unless the output is completely decoupled from the control input,  $d$  is finite, and hence, (5) is well-defined.

Recall that the relative degree  $d$  determines the lag from the inputs to the outputs in a control system (1). In particular, the first instance of the output signal which is affected by  $u_0$  is  $y_{d+1} = h_i(x_{d+1})$ . Hence, by definition (5),

$$\frac{\partial \hat{h}_i(x_t, u_t)}{\partial u_t} \neq 0$$

holds and the new output functions  $\hat{h}_i$  satisfy Assumption 3. The transform in (5) can be understood as a mere forward time shift,

$$\hat{h}_i(x_t, u_t) = h_i(x_{t+d+1}) \quad (6)$$

Therefore, by replacing the output functions  $h_i$  by  $\hat{h}_i$  in (2), the same constraints are imposed on  $y_{i,t}$  starting from  $t = d + 1$ . The  $d$  first steps of the optimal control problem, where the original output constraint is not enforced, is often negligible, especially when the sampling time of the system is small (see § 4).

**Remark 1.** *The family of monotone dynamical systems defined by Assumptions 2 and 3 is closely related to several other families of systems studied in the literature,*

*such as incrementally positive systems [2], monotone control systems [2], and positive systems [8]. In particular, if  $f(0, 0) = 0$ ,  $h(0, 0) = 0$  and Assumption 2 holds, the system (1) is a discrete-time internally positive control system in the sense of [9]. If, in addition,  $f$  and  $h$  are linear, the dynamical system (1) can describe all linear time-invariant internally positive systems that have a single input and are not strictly proper. Strictly proper systems can also be handled as long as their outputs are not completely decoupled from the input, by modifying the output functions as in (5).*

### 3 SOLUTION METHODS

In this section, we study solutions to the optimization problem (2) and propose a few different techniques to find and implement the optimal control input  $u^*$  in (2).

#### 3.1 Open-loop sequences

The traditional way to approach discrete-time optimal control problems is to apply generic nonlinear programming techniques, such as sequential quadratic programming, to find a feasible sequence of control inputs  $u = \{u_t\}_{t=0}^{t=t_f}$  that attains a large objective value. However, it is, in general, difficult to guarantee that an optimal solution will be found, or even to validate that a feasible control sequence is globally optimal.

The problem is simplified when the transition function  $f$  is linear. In this case, as long as the output functions  $h_i(x)$  are convex and the running costs  $L(x, u)$  are concave functions of their arguments, the optimal control problem (2) can be posed as a standard convex optimization problem with  $(n+1)t_f + 1$  variables and  $(t_f+1)(p+1) + t_f$  constraints. The optimal control sequence can then be computed efficiently using a wide range of reliable numerical routines.

While this approach has some merits, it finds an open-loop control sequence, and is therefore sensitive to model uncertainties and fragile to use in practice.

#### 3.2 Closed-loop policies

To obtain a more robust control policy, it is beneficial to describe the optimal solution  $u^*$  of (2) as a feedback policy. The next lemma is a first step towards such policies. It reveals that the optimal control sequence seeks to achieve input maximization and constraint activation.

**Lemma 1.** *Under Assumptions 1–3, the following two statements hold for the optimal control problem (1)–(2):*

- 1) *There is an optimal solution  $u^*$  to problem (2) that cannot be increased at any single time  $t \in [0, t_f]$ .*
- 2) *Under this optimal solution, at least one inequality constraint in (2) is active at  $t = t_f$ .*

*Proof.* Let  $u^*$  be an optimal solution to the optimal control problem (1)-(2). Define another input sequence  $\hat{u}(\varepsilon) = \{\hat{u}_t\}_{t=0}^{t=t_f}$  by increasing  $\hat{u}^*$  at a single time  $\tau \in [0, t_f]$ ,

$$\hat{u}_t = \begin{cases} u_t^* + \varepsilon, & t = \tau \\ u_t^*, & t \neq \tau \end{cases} \quad (7)$$

where  $\varepsilon \geq 0$ . Let  $x^* = \{x_t^*\}_{t=0}^{t=t_f}$  and  $\hat{x}(\varepsilon) = \{\hat{x}_t\}_{t=0}^{t=t_f}$  denote the state trajectories of the system (1) associated with the control inputs  $u^*$  and (7) respectively. As (1) is causal, the trajectory  $\hat{x}(\varepsilon)$  associated with  $\hat{u}(\varepsilon)$  satisfies

$$\hat{x}_t = x_t^*, \quad t = 0, 1, \dots, \tau$$

We will now use induction to show that the monotonicity of the system (Assumption 2) implies that

$$\hat{x}_t \geq x_t^*, \quad t = \tau + 1, \dots, t_f \quad (8)$$

To this end, first note that since  $\hat{u}_\tau \geq u_\tau^*$  and the function  $f$  is increasing in the second argument, inequality (8) holds for  $t = \tau + 1$  because

$$\hat{x}_{\tau+1} = f(\hat{x}_\tau, \hat{u}_\tau) \geq f(x_\tau^*, u_\tau^*) = x_{\tau+1}^*$$

Moreover, if (8) holds for some  $t \in [\tau + 1, t_f - 1]$ , then

$$\hat{x}_{t+1} = f(\hat{x}_t, \hat{u}_t) \geq f(x_t^*, u_t^*) = x_{t+1}^*$$

since  $f$  is increasing in its first argument. This proves that (8) holds for all  $\tau + 1 \leq t \leq t_f$ . Next, define

$$\begin{aligned} \Delta(\varepsilon) &= J(x_0, \hat{u}(\varepsilon)) - J(x_0, u^*) \\ &= \sum_{t=0}^{\tau} L(\hat{x}_t, \hat{u}_t) - \sum_{t=0}^{\tau} L(x_t^*, u_t^*). \end{aligned} \quad (9)$$

Note that  $\Delta(0) = 0$  since  $\hat{u}(0) = u^*$ , and that the monotonicity of the running costs implies that  $\Delta(\varepsilon) \geq 0$ . On the other hand, optimality of  $u^*$  means that  $\Delta(\varepsilon) \leq 0$ , but there could be a range of  $\varepsilon$ -values for which the quantity remains at zero. Let us define  $\bar{\varepsilon} \in [0, u_{\max} - u_\tau^*]$  as the largest value of  $\varepsilon$  such that  $\hat{x}(\varepsilon)$  is feasible and  $\Delta(\varepsilon) = 0$  for all  $\varepsilon \in [0, \bar{\varepsilon}]$ . Such a maximal value  $\bar{\varepsilon}$  exists because  $\Delta(0) = 0$  and  $\Delta(\varepsilon)$  is continuous in  $\varepsilon$  (since  $L$  is continuous). Clearly,  $\hat{u}(\varepsilon)$  is also optimal, and cannot be increased at time  $\tau$ . By repeating the same process with  $\hat{u}(\bar{\varepsilon})$  as starting point, one can find an optimal solution that is maximal at every time step. This proves point 1.

Now let  $u^*$  be the optimal solution that is maximal at every time step. For any  $\tau \in \{0, 1, \dots, t_f\}$ , an increment in  $u_\tau^*$  (while keeping the equality constraints (1) satisfied and keeping  $u_t^*$  constant for all  $t \neq \tau$ ) will violate at least one constraint in the optimal control problem (2). Since the system (1) is causal, the violation must occur at some  $t^* \in \{\tau, \tau + 1, \dots, t_f\}$ . Since the function  $f$  is

continuous (Assumption 2), the increment in  $u_\tau^*$  and  $x_{t^*}^*$  can be chosen arbitrarily small. As the output function  $h$  is also continuous (Assumption 3), the increments in  $y_{i,t^*} = h_i(x_{t^*}^*, u_{t^*}^*)$  can be made as small as desired, and still violate one of the inequality constraints in (2). This indicates that the corresponding constraint is active under the optimal control sequence  $u^*$ . Finally, as the above argument holds for any  $\tau \in [0, t_f]$ , one may choose  $\tau = t_f$  which gives  $t^* = t_f$ . This proves point 2.  $\square$

For some families of monotone optimal control problems, the optimal solution does not only activate inequality constraints at some time instant but makes at least one inequality constraint active at every time instant  $t \in [0, t_f]$ . One such family is introduced next.

**Theorem 1.** *Let Assumptions 1–3 hold. In addition, assume that the output function  $h(x_t, u_t)$  is differentiable and decreasing in  $x_t$  and  $\partial h_i(x_t, u_t)/\partial u_t \neq 0$  for all  $x_t \in \mathcal{R}(x_0, t_f)$  and  $u_t \in (-\infty, u_{\max}]$ . Then there is an optimal solution  $u^*$  of problem (2) that makes at least one inequality constraint active at every time step  $t \in [0, t_f]$ .*

*Proof.* For ease of exposition, we merge the input and output inequality constraints in Problem (2) by defining

$$y_{0,t} = h_0(x_t, u_t) = u_t \quad \text{and} \quad y_{0,\max} = u_{\max}$$

Let  $\mathcal{I}_t$  denote the set of indices  $i$  such that  $y_{i,t} = y_{i,\max}$  holds under the optimal trajectory. We will use induction to prove that  $\mathcal{I}_t$  is non-empty for every  $t \in [0, t_f]$ . First, by Lemma 1 there is at least one inequality constraint active at time  $t = t_f$  under the optimal sequence  $u^*$ , which implies that  $\mathcal{I}_{t_f} \neq \emptyset$ . Now assume that

$$\mathcal{I}_t \neq \emptyset, \quad \forall t \in [\tau + 1, t_f] \quad (10)$$

for some  $\tau \in [0, t_f - 1]$ . Equation (18) means there is at least one active inequality constraint at each time step in  $t \in [\tau + 1, t_f]$ . Then we show that there is also an inequality constraint active at time  $t = \tau$ , *i.e.*

$$\mathcal{I}_\tau \neq \emptyset.$$

Define a control sequence  $\hat{u}(\varepsilon) = \{\hat{u}_t\}_{t=0}^{t=t_f}$  by perturbing the optimal solution  $u^*$  as

$$\hat{u}_t = \begin{cases} u_t^* + \varepsilon_t, & t \geq \tau \\ u_t^*, & t < \tau \end{cases} \quad (11)$$

where  $\varepsilon_\tau > 0$ . Let the perturbations  $\varepsilon \in \mathbb{R}^{t_f - \tau + 1}$  be chosen such that the active constraints in the range  $t \in [\tau + 1, t_f]$  remain active under the new control sequence

$\hat{u}(\varepsilon)$ . This happens if for all  $t \in [\tau + 1, t_f]$  and  $i \in \mathcal{I}_t$ ,

$$\begin{aligned} dy_{i,t} = & \quad (12) \\ & \frac{\partial h_i(x_t, u_t)}{\partial u_t} \varepsilon_t + \frac{\partial h_i(x_t, u_t)}{\partial x_t} \frac{\partial f(x_{t-1}, u_{t-1})}{\partial u_{t-1}} \varepsilon_{t-1} + \\ & \sum_{k=\tau}^{t-2} \frac{\partial h_i(x_t, u_t)}{\partial x_t} \left( \prod_{j=t-1}^{k+1} \frac{\partial f(x_j, u_j)}{\partial x_j} \right) \frac{\partial f(x_k, u_k)}{\partial u_k} \varepsilon_k = 0 \end{aligned}$$

as  $\varepsilon \rightarrow 0$ , where all the partial derivatives are evaluated along the optimal trajectory  $x = x^*$  and  $u = u^*$ . Now we show that equation (12) yields

$$\varepsilon_k \geq 0, \quad k = \tau, \tau + 1, \dots, t_f \quad (13)$$

by induction. Starting with  $t = \tau$ , one has  $\varepsilon_k > 0$  by definition (11). Assuming that (13) holds for all  $k \in \{\tau, \dots, t-1\}$ , one has

$$\begin{aligned} & \frac{\partial h_i(x_t, u_t)}{\partial u_t} \varepsilon_t = \\ & - \sum_{k=\tau}^{t-1} \frac{\partial h_i(x_t, u_t)}{\partial x_t} \left( \prod_{j=t-1}^{k+1} \frac{\partial f(x_j, u_j)}{\partial x_j} \right) \frac{\partial f(x_k, u_k)}{\partial u_k} \varepsilon_k \end{aligned}$$

from (12), which is non-negative due to Assumption 2 and the fact that  $h(x_t, u_t)$  is decreasing in  $x_t$ . Therefore, as  $\partial h_i(x_t, u_t)/\partial u_t > 0$ , one obtains  $\varepsilon_t \geq 0$ . This proves (13). Consider the first-order perturbation of the cost function as

$$\begin{aligned} \Delta(\varepsilon) &= J(x_0, \hat{u}(\varepsilon)) - J(x_0, u^*) = \\ &= \sum_{t=\tau}^{t_f} \frac{\partial L(x_t, u_t)}{\partial u_t} \varepsilon_t \\ &+ \sum_{k=0}^{t_f-\tau-1} \sum_{t=\tau}^{t_f-k-1} \frac{\partial L(x_{t+k+1}, u_{t+k+1})}{\partial x_{t+k+1}} \times \\ &\left( \prod_{j=t+k}^{j=t+1} \frac{\partial f(x_j, u_j)}{\partial x_j} \right) \frac{\partial f(x_t, u_t)}{\partial u_t} \varepsilon_t. \quad (14) \end{aligned}$$

where all the partial derivatives are evaluated along the optimal trajectory  $x = x^*$  and  $u = u^*$ . Since all the terms in (14) are non-negative by (13) and Assumptions 2 and 1,

$$\Delta(\varepsilon) \geq 0 \quad (15)$$

holds true. Two cases are possible based on (15).

*Case 1:*  $J(x_0, \hat{u}(\varepsilon)) > J(x_0, u^*)$  holds in a neighborhood of  $\varepsilon = 0$ . In this case  $\hat{u}(\varepsilon)$  is infeasible (since  $u^*$  is assumed to be an optimal solution), which means  $\hat{u}(\varepsilon)$  violates at least one inequality constraint. Since system (1) is causal, the violated constraint must occur at some  $t^* \in \{\tau, \dots, t_f\}$ . However, as the active constraints in the range  $t \in \{\tau + 1, \dots, t_f\}$  are kept satisfied under the

perturbed input sequence  $\hat{u}(\varepsilon)$ , the violated constraint must occur at  $t = \tau$ .

*Case 2:*  $J(x_0, \hat{u}(\varepsilon)) = J(x_0, u^*)$  holds for some  $\varepsilon$ . This case implies that the sequence  $\hat{u}(\varepsilon)$  is also an optimal solution to Problem 2 which satisfies

$$\hat{u}_\tau > u_\tau^*$$

Using the new optimal sequence  $\hat{u}(\varepsilon)$  as the starting point and repeating the same process described above, one can obtain an optimal sequence that makes an inequality constraint active at  $t = \tau$ , because  $h_i(x_\tau, u_\tau)$  is strictly increasing in  $u_\tau$  for all  $i$  (Assumption 3).

We have shown that an inequality constraint is active at  $t = \tau$ , if there is an inequality constraint active at each  $t \in [\tau + 1, t_f]$ . The proof is complete by induction.  $\square$

The optimal input sequences introduced in Theorem 1 are called *bang-ride* in the literature since they either use the maximal input or “ride” the output constraint boundaries. As we will show later, these solutions are desirable since they enable a simple feedback implementation. Another family of optimal monotone problems with bang-ride optimal solutions is introduced next. This family does not require the output maps to be decreasing in  $x$  and finds important applications in the fast-charging problems considered in Section 4.

**Theorem 2.** *Let Assumptions 1–3 hold. In addition, assume that the functions  $f, h, L$  are linear, i.e.*

$$\begin{aligned} f(x_t, u_t) &= Ax_t + Bu_t \\ h(x_t, u_t) &= Cx_t + Du_t \\ L(x_t, u_t) &= Ex_t + Fu_t \end{aligned} \quad (16)$$

If the impulse response of (1)

$$g_t = \begin{cases} D, & t = 0 \\ CA^{t-1}B, & t \geq 1 \end{cases} \quad (17)$$

is decreasing in the range  $t \in [0, t_f]$ , then there is an optimal solution  $u^*$  of (1)-(2) that makes at least one inequality constraint active at every time step  $t \in [0, t_f]$ .

*Proof.* The proof follows a similar set of arguments as the proof of Theorem 1. First, we merge the input and output inequality constraints in problem (2) by defining

$$y_{0,t} = h_0(x_t, u_t) = u_t \quad \text{and} \quad y_{0,\max} = u_{\max}$$

Let  $\mathcal{I}_t$  denote the set of indices  $i$  such that  $y_{i,t} = y_{i,\max}$  holds under the optimal trajectory. We will use induction to prove that  $\mathcal{I}_t$  is non-empty for every  $t \in [0, t_f]$ . First, we note that by Lemma 1,  $\mathcal{I}_{t_f} \neq \emptyset$ . Now assume that

$$\mathcal{I}_t \neq \emptyset, \quad \forall t \in [\tau + 1, t_f] \quad (18)$$

for some  $\tau \in [0, t_f - 1]$ . We will show that there is then also an inequality constraint active at time  $t = \tau$ , *i.e.*

$$\mathcal{I}_\tau \neq \emptyset.$$

Define a control sequence  $\hat{u}(\varepsilon) = \{\hat{u}_t\}_{t=0}^{t_f}$  by perturbing the optimal solution  $u^*$  as in (11) using some  $\varepsilon_\tau > 0$ . Let the perturbations  $\varepsilon \in \mathbb{R}^{t_f - \tau + 1}$  be chosen such that the active constraints in the range  $t \in [\tau + 1, t_f]$  remain active under the new control sequence  $\hat{u}(\varepsilon)$ . This happens if (12) holds for all  $t \in [\tau + 1, t_f]$  and  $i \in \mathcal{I}_t$ , which in the linear case (16) yields

$$\begin{aligned} dy_{i,t} &= D_i \varepsilon_t + \sum_{k=\tau}^{t-1} C_i A^{t-k-1} B \varepsilon_k \\ &= \sum_{k=\tau}^t g_{i,t-k} \varepsilon_k = 0 \end{aligned} \quad (19)$$

as  $\varepsilon \rightarrow 0$ . Applying Abel's transform to (19) gives

$$g_{i,0} \sigma_{t-\tau} = \sum_{k=0}^{t-\tau-1} (g_{i,t-\tau-k-1} - g_{i,t-\tau-k}) \sigma_k \quad (20)$$

where

$$\sigma_k = \sum_{j=\tau}^{\tau+k} \varepsilon_j.$$

Now since  $g_{i,0} = D_i > 0$  (by Assumption 3),  $g_{i,t}$  is a decreasing function of  $t$  and  $\sigma_0 = \varepsilon_\tau > 0$ , setting  $t = \tau + 1$  in (20) gives  $\sigma_1 \geq 0$ . Similarly, by setting  $t = \tau + 2, \tau + 3, \dots, t_f$  in (20) it is deduced that

$$\sigma_k \geq 0, \quad k = 0, 1, \dots, t_f - \tau \quad (21)$$

The first-order perturbation in the cost function is then given by (14), which by assuming (16) takes the form

$$\begin{aligned} \Delta(\varepsilon) &= J(x_0, \hat{u}(\varepsilon)) - J(x_0, u^*) = \\ &= \sum_{t=\tau}^{t_f} F \varepsilon_t + \sum_{k=0}^{t_f - \tau - 1} \sum_{t=\tau}^{t_f - k - 1} E A^k B \varepsilon_t \\ &= F \sigma_{t_f - \tau} + \sum_{k=0}^{t_f - \tau - 1} E A^k B \sigma_{t_f - k - 1 - \tau} \end{aligned} \quad (22)$$

where all the matrix coefficients are non-negative due to Assumptions 2 and 1. As all  $\sigma_k$ 's are non-negative, the summands in (22) are non-negative and

$$\Delta(\varepsilon) \geq 0 \quad (23)$$

holds true. The rest of the proof is identical to that of Theorem 1 and hence omitted.  $\square$

The optimality of bang-ride policies has been proven for specific systems [14] and conjectured for others [12]. However, to the best of our knowledge, Theorems 1 and 2 are the first results that establish the bang-ride property of the optimal control for large classes of systems.

Note that the additional requirement of a decreasing impulse response is essential in Theorem 2. The monotonicity Assumptions 1–3 and linearity of the functions (16) do not alone guarantee that a bang-ride solution is optimal. To prove this claim, consider an instance of (2) where the dynamics and running costs are linear and the matrices in (16) are all non-negative. Furthermore, let  $x_0 = 0$ ,  $t_f = 1$ ,  $u_{\max} > 0$ ,  $y_{\max} = D u_{\max}$ ,  $E = 0$  and  $F = 1$ . The constraints for this problem are

$$\begin{aligned} (u_0 \leq u_{\max}) \wedge (y_0 = D u_0 \leq y_{\max}) & \quad (t = 0) \\ (u_1 \leq u_{\max}) \wedge (y_1 = C B u_0 + D u_1 \leq y_{\max}) & \quad (t = 1) \end{aligned}$$

The two constraints at  $t = 0$  are equivalent, and a bang-ride solution  $u_{\text{br}} = \{u_0, u_1\}$  must have  $u_0 = u_{\max}$ . We can therefore re-write the constraints at  $t = 1$  as

$$(u_1 \leq u_{\max}) \wedge (D u_1 \leq (D - C B) u_{\max}) \quad (24)$$

Define

$$\gamma = \min_i \{ [D - C B]_i / [D]_i \}$$

where  $[\cdot]_i$  denotes the  $i$ th component. Since the system is positive, we have  $\gamma \leq 1$ . Therefore,  $u_1 = \gamma u_{\max}$  holds for any bang-ride solution satisfying (24). The total cost of  $u_{\text{br}}$  is

$$J(0, u_{\text{br}}) = u_0 + u_1 = (1 + \gamma) u_{\max}$$

Now consider another control sequence  $u = \{0, u_{\max}\}$ . It is easy to show that this control sequence is feasible and  $J(0, u) = u_{\max}$ . Comparing the two costs yields

$$J(0, u_{\text{br}}) - J(0, u) = \gamma u_{\max}$$

Hence, if  $\gamma < 0$ , which corresponds to  $D < C B$  and thereby to an increasing impulse response in the range  $t \in \{0, 1\}$ , then the bang-ride control is *not* optimal.

Whenever a monotone optimal control problem has an optimal solution of bang-ride type, it is easy to determine an optimal state feedback policy. To see this, we first note that since the output functions are strictly increasing, each constraint equation

$$h_i(x_t, u_t) = y_{i,\max}, \quad i = 1, 2, \dots, p \quad (25)$$

has at most one solution as  $u_t = K_i(x_t)$  where  $K_i : \mathbb{R}^n \rightarrow \mathbb{R}$  is a possibly nonlinear function. By defining  $K_i(x_t) = +\infty$  in case the equation (25) has no real solution for  $u_t$ ,

it is possible to write the bang-ride control law as the following nonlinear state-feedback

$$u_t = \min\{K_0(x_t), K_1(x_t), \dots, K_p(x_t)\} \quad (26)$$

where  $K_0(x_t) = u_{\max}$  corresponds to the only input constraint in (2). As  $K_0(x_t)$  is finite, the control law (26) is always well-defined.

**Proposition 1.** *The control sequence (26) satisfies the optimality conditions of Lemma 1.*

*Proof.* Let  $i^* = \arg \min_i \{K_i(x_t)\}$ . In case  $i^* = 0$ , one has  $u_t = u_{\max}$  which means the input constraint in (2) is active. Otherwise when  $i^* > 0$ , the output constraint  $h_{i^*}(x_t, u_t) = y_{i^*, \max}$  is active under the control sequence (26) and assuming  $u_t > \min_i \{K_i(x_t)\} = K_{i^*}(x_t)$  results in the following inequality

$$h_{i^*}(x_t, u_t) > h_{i^*}(x_t, K_{i^*}(x_t)) = y_{i^*, \max}$$

from (4). Therefore, increasing  $u_t$  in (26) is infeasible.  $\square$

When the system model (1) is known, it is usually possible to solve the equations (25) analytically to obtain or approximate the feedback functions  $K_i$ . In the linear case (16) for example,  $K_i$  are simply given by

$$K_i(x_t) = (y_{i, \max} - C_i x_t) / D_i$$

where  $C_i$  and  $D_i$  denote the  $i$ th rows of matrices  $C$  and  $D$ . In the general case, one can use techniques such as the Lagrange inversion theorem to determine the functions  $K_i$ . Alternatively, one can solve the equations (25) numerically, using standard root-finding algorithms. Unlike the analytic approach, which can be executed offline, the numerical approach requires that the equations (25) are solved online in every iteration. Typical numerical methods for solving (25) include Newton's method when the output functions have continuous derivatives.

The closed-loop policy discussed above has the advantage of being more robust to model uncertainties than the open-loop policy. However, it requires full state measurements to generate the control signal, which limits its value to applications where only certain outputs are measured by sensors.

### 3.3 Heuristic selector control strategies

The optimal control policy (26) has an interesting structural property. It uses  $p + 1$  controllers, each designed to keep a corresponding signal at a constraint boundary, and activates (selects) the controller that produces the smallest control signal. In an output feedback setting, where only the process outputs are measured, it is logical to retain this structure. When we have a good model

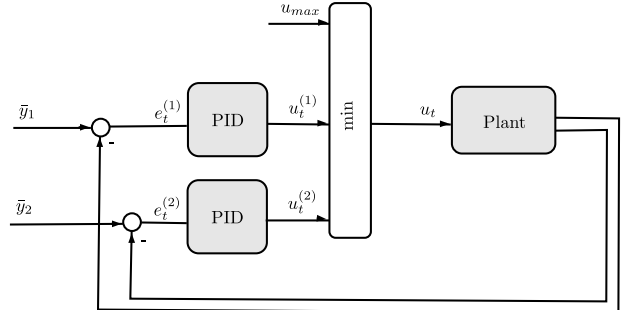


Fig. 1. Selector control structure for a system with  $p = 2$ . The anti-windup feedback links are not shown in this figure.

of the process dynamics one can, for example, estimate the state vector using an observer and replace the true states in (26) with estimated ones. When we lack a good process model, on the other hand, we may try to replace the state feedback laws in (26) with simple output feedback controllers, such as PID.

Figure 1 shows a selector control structure for the system (1) which has one input and  $p = 2$  outputs. There is a total of  $p$  PID control loops, one for each output in (1). However, only one loop is connected at each time step. The active loop is chosen by the min selector device. This separation of the output channels simplifies the controller design significantly, as one can tune each set of PID parameters separately based on the isolated single-input-single-output feedback loop.

There are several considerations for tuning the PID controllers present in the selector control structure that approximates the monotone optimal control policy. Among the available PID tuning methods, the rules that are based on observing a system response are particularly attractive, since making a single step in the input signal and observing the  $p$  outputs allows for tuning of all controllers based on only one experiment. For the design specification, special attention is paid to setpoint following. The reason is that the occurrence of an overshoot in the  $i^{\text{th}}$  loop implies that  $y_{i,t} > y_{i, \max}$ , i.e. a constraint violation in (2). In addition, a slow response is undesirable since it leads to a large optimality gap  $|y_{i, \max} - y_{i,t}|$  where  $y_{i,t}^* = y_{i, \max}$  is the  $i^{\text{th}}$  system output under the optimal control sequence and  $i$  is the active constraint in the optimal trajectory at time  $t$ . Based on the above arguments, a suitable control design technique for the selector control loops should minimize overshoots and seek a fast response. Several tuning methods are available that account for these considerations [4]. One such method is [20] which relies on the first few impulse-response samples of the plant and provides a set of gains that are known to promote the positivity of the tracking error and reduce overshoots.

Another complication that arises in selector control is integrator windup in the PID blocks when the loops

switch. However, this problem can be easily treated using a back-calculation technique [3, §3.5], which results in the following control signals generated by the PID controllers:

$$u_t^{(i)} = k_i^p e_t^{(i)} + k_i^I \sum_{k=0}^{t-1} e_k^{(i)} + k_i^d (e_t^{(i)} - e_{t-1}^{(i)}) + k_i^w \sum_{k=0}^{t-1} u_k - u_k^{(i)}$$

for all  $i = 1, 2, \dots, p$ , where  $e_t^{(i)} = y_{i,\max} - y_{i,t}$  and  $k_i^w$  is the anti-windup gain. When  $k_i^w = 0$  there is no anti-windup in operation and the  $i^{\text{th}}$  controller falls back to a basic PID. The following control input  $u$  is fed to the system (1) from the selector device:

$$u_t = \min\{u_{\max}, u_t^{(1)}, \dots, u_t^{(p)}\}, \quad t \in \mathbb{N}_0 \quad (27)$$

## 4 APPLICATION TO FAST CHARGING

In this section, we will demonstrate how the result developed in Sections 2 and 3 can be applied to the design of fast-charging protocols for electrical batteries. Fast charging of lithium-ion batteries in a way that limits degradation is a challenging task that has received recent attention in the research community; see the review [5]. The standard battery charging protocol constant-current-constant-voltage (CCCV) used in the industry is of bang-ride form, as it starts charging the battery with the maximum current and then adapts the charging current to keep the voltage across the battery constant. The bang-ride behavior is also observed in some optimization problems that describe fast-charging for different battery models. For example, a bang-ride solution was obtained from the application of nonlinear model predictive control to a fast-charging problem that involves a multi-physics circuit battery model [12]. Bang-ride solutions were also proven to be optimal using Pontryagin's principle for three single-particle battery models in [14] and for an equivalent circuit battery model in [1]. However, as demonstrated in [10], for example, not every battery model and not every fast-charging problem formulation admits an optimal solution that is of bang-ride type. The results of Section 3 can be used to identify those fast-charging problems whose optimal solutions are bang-ride.

Several battery models and optimal control formulations have been studied for health-aware fast-charging of lithium-ion batteries. As it was demonstrated in [6], many of these problems satisfy monotonicity assumptions similar to those stated in Section 2 and can therefore be treated as monotone optimal control problems. This allows applying Lemma 1 and Theorems 1 and 2 to these problems and implement their optimal solutions

by selector control strategies. We demonstrate this approach on two different battery models in this section.

### 4.1 Single-Particle Models (SPM)

Single-Particle Models (SPM) are perhaps the most common reduced-order electrochemical models used for lithium-ion batteries. A continuous-time SPM derived from a third-order Padé approximation of the diffusion equation that describes the intercalation process and mass transport in the electrodes is given by the following state-space equations [14]

$$\begin{aligned} \dot{x}_1(t) &= -a_1 x_1(t) + b_1 u^-(t) \\ \dot{x}_2(t) &= -a_2 x_2(t) - b_2 u^-(t) \\ \dot{x}_3(t) &= -b_3 u^-(t) \\ y(t) &= -c_1 x_1(t) + c_2 x_2(t) + c_3 x_3(t) \end{aligned} \quad (28)$$

where  $u^-$  is the discharging current,  $x_3$  is the bulk concentration for the anode,  $y$  is the surface concentration, and all the coefficients  $a_1, a_2, b_1, b_2, b_3, c_1, c_2, c_3$  are positive. After the change of coordinates suggested in [6] and defining  $u(t) = -u^-(t)$ , we obtain the model

$$\begin{aligned} \dot{x}_1(t) &= -a_1 x_1(t) + b_1 u(t) \\ \dot{x}_2(t) &= -a_2 x_2(t) + b_2 u(t) \\ \dot{x}_3(t) &= b_3 u(t) \\ y(t) &= c_1 x_1(t) + c_2 x_2(t) + c_3 x_3(t) \end{aligned}$$

Euler discretization results in the discrete-time model

$$\begin{aligned} x_{t+1} &= Ax_t + Bu_t \\ h(x_t, u_t) &= Cx_t \end{aligned} \quad \text{for } t \in \mathbb{N}_0, \quad (29)$$

where

$$A = \begin{bmatrix} 1 - a_1 t_s & 0 & 0 \\ 0 & 1 - a_2 t_s & 0 \\ 0 & 0 & 1 \end{bmatrix}, \quad B = \begin{bmatrix} b_1 t_s \\ b_2 t_s \\ b_3 t_s \end{bmatrix}, \quad C = \begin{bmatrix} c_1 \\ c_2 \\ c_3 \end{bmatrix}^T$$

A fast-charging problem was proposed in [14] based on (28) to maximize the bulk concentration at the anode while restricting both the surface concentration and the charging current. For the discretized model (29), this optimal control problem can be written as

$$\begin{aligned} &\underset{u}{\text{maximize}} \quad J(x_0, u) = \sum_{t=0}^{t_f} x_{3,t} \\ &\text{subject to} \quad y_t \leq y_{\max}, \\ &\quad u_t \leq u_{\max}, \\ &\quad x_{t+1} = Ax_t + Bu_t, \\ &\quad y_t = \hat{C}x_t + \hat{D}u_t \end{aligned} \quad (30)$$



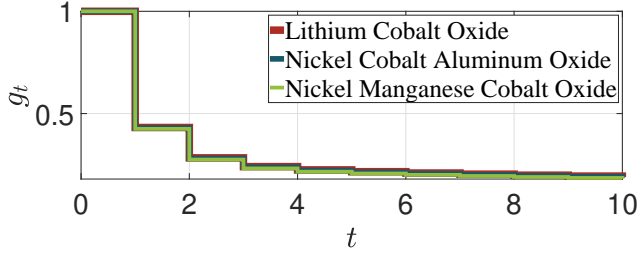


Fig. 2. Normalized impulse responses of three batteries with different chemistries [14, 15].

Here, since the system model (29) does not have a direct feedthrough to the outputs, we have used the approach in (5) to redefine the output functions as

$$y_t = \hat{h}(x_t, u_t) = CAx_t + CBu_t := \hat{C}x_t + \hat{D}u_t \quad (31)$$

Since  $\hat{D} = CB > 0$ , Assumption 3 is satisfied in (30). Moreover, by choosing a sampling time in the range

$$t_s \in (0, 1/\max\{a_1, a_2\}], \quad (32)$$

Assumption 2 is also satisfied. Therefore, the optimal control problem (30) satisfies Assumptions 1, 2, 3 and, according to Theorem 2, the optimal charging protocol in (30) is bang-ride if

$$g_t = \begin{cases} \hat{D}, & t = 0 \\ \hat{C}A^{t-1}B, & t \geq 1 \end{cases} \quad (33)$$

is decreasing in the range  $t \in [0, t_f]$ . This is true for all the three sets of battery parameters considered in [14, 15], as shown in Figure 2. Therefore, the optimal charging protocol for these battery models is bang-ride, a result that is consistent with [14]. In contrast with [14], our results allow to prove optimality for *all* SPM battery model parameters  $a_1, a_2, b_1, b_2, b_3, c_1, c_2, c_3$  that result in a decreasing impulse response  $g_t$ .

#### 4.2 Equivalent-Circuit Models (ECMs)

Equivalent-Circuit Models (ECMs) are one of the most popular empirical models of lithium-ion battery cells [13]. A continuous-time ECM with two time constants is given by the following set of ordinary differential equations

$$\begin{aligned} \dot{v}_1(t) &= -\frac{1}{R_1C_1}v_1(t) + \frac{1}{C_1}u(t) \\ \dot{v}_2(t) &= -\frac{1}{R_2C_2}v_2(t) + \frac{1}{C_2}u(t) \\ \dot{s}(t) &= \frac{1}{Q}u(t) \\ y(t) &= v_1(t) + v_2(t) + \beta s(t) + R_0u(t) \end{aligned} \quad (34)$$

Here,  $u$  is the charging current,  $v_1, v_2$  are the voltages across the (abstract) RC-links,  $s$  is the state of charge, and  $y$  is the over-potential voltage. This model is based on the assumption that the open-circuit voltage function of the battery is known and the state of charge can be computed via integration of the input current  $u$ . A forward Euler discretization of (34) with sampling time  $t_s$  yields in the following discrete-time battery model

$$\begin{aligned} x_{1,t+1} &= (1 - t_s/(R_1C_1))x_{1,t} + \frac{t_s}{C_1}u_t \\ x_{2,t+1} &= (1 - t_s/(R_2C_2))x_{2,t} + \frac{t_s}{C_2}u_t \\ x_{3,t+1} &= x_{3,t} + \frac{t_s}{Q}u_t \\ h(x_t, u_t) &= x_{1,t} + x_{2,t} + \beta x_{3,t} + R_0u_t \end{aligned} \quad (35)$$

We assume  $x_0 = 0$  as the initial condition. Now consider the fast charging problem (2) with the cost function:

$$L(x_t, u_t) = x_{3,t}. \quad (36)$$

which maximizes the stored battery capacity at the end of the charge. We consider constraints on the cell's charging current  $u_t$  as well as its over-potential voltage  $y_t = h(x_t, u_t)$ . In particular, constraining the over-potential rather than the terminal voltage (as in conventional CCCV protocols) helps prevent stress and strain [1]. In general, these constraints are known to promote safety and limit degradation [7] and can be written as

$$\begin{aligned} u_t &\leq u_{\max}, \\ y_t &\leq y_{\max} \end{aligned}$$

for some positive constants  $u_{\max}$  and  $y_{\max}$ . By choosing a sampling time  $t_s \in (0, t_s^{(1)})$ , where

$$t_s^{(1)} = \min\{R_1C_1, R_2C_2\} \quad (37)$$

the transition function  $f(x_t, u_t)$  is increasing in both  $x_t$  and  $u_t$ . It is also obvious that  $f(x_t, u_t)$  is continuous everywhere. Therefore, Assumption 2 is satisfied. It can similarly be shown that Assumptions 1 and 3 are also satisfied. Therefore, the fast charging problem described above is a monotone optimal control problem, and its optimal solution satisfies the input maximization property described in Lemma 1. By further restricting the sampling time to  $t_s \in (0, \min\{t_s^{(1)}, t_s^{(2)}\}]$ , where

$$t_s^{(2)} = \frac{R_0}{\frac{1}{C_1} + \frac{1}{C_2} + \frac{\beta}{Q}} \quad (38)$$

the (more restrictive) hypothesis of Theorem 2 is also satisfied. To see this, we first note that both the cost function (36) and the process dynamics (35) are linear

with the impulse response satisfying  $g_0 = R_0$  and

$$g_t = \frac{\left(1 - \frac{t_s}{R_1 C_1}\right)^{t-1}}{C_1/t_s} + \frac{\left(1 - \frac{t_s}{R_2 C_2}\right)^{t-1}}{C_2/t_s} + \frac{t_s \beta}{Q}$$

for  $t \geq 1$ . Since  $0 < t_s \leq t_s^{(2)}$  implies

$$g_0 = R_0 \geq \frac{t_s}{C_1} + \frac{t_s}{C_2} + \frac{t_s \beta}{Q} = g_1$$

and  $0 < t_s \leq t_s^{(1)}$  ensures  $g_t$  is always decreasing in the range  $t \in [1, t_f]$  for any  $t_f \geq 1$ . Therefore, if

$$t_s \in (0, \min\{t_s^{(1)}, t_s^{(2)}\})$$

then the impulse response is decreasing in  $t \in [0, t_f]$  and the monotone optimal control problem considered here also satisfies the hypothesis of Theorem 2. This indicates that the optimal solution is of bang-ride form and can be implemented using selector control.

Hence, to compute the optimal closed-loop policy, one may solve the constraint equations (25) analytically to obtain

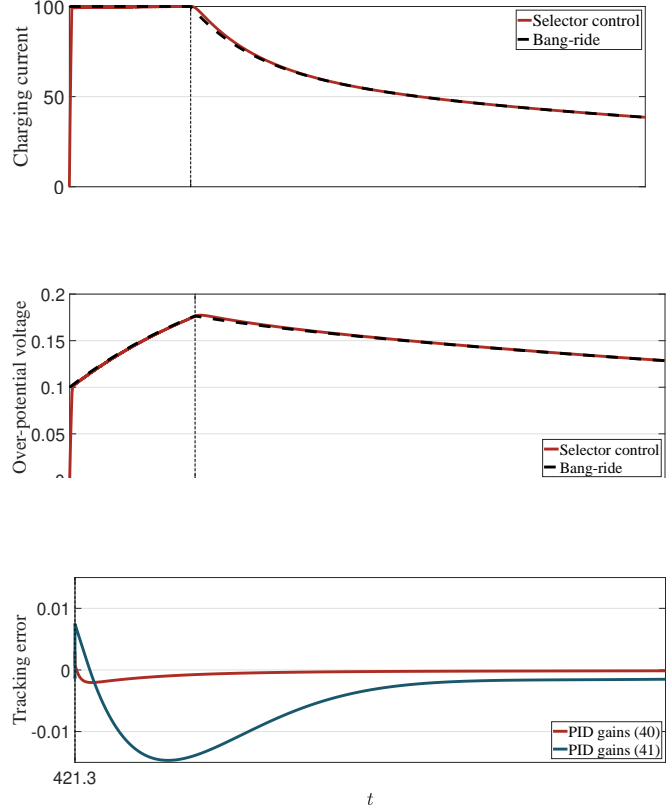
$$\begin{aligned} K_0(x_t) &= u_{\max} \\ K_1(x_t) &= (y_{\max} - x_{1,t} - x_{2,t} - \beta x_{3,t})/R_0 \end{aligned} \quad (39)$$

Alternatively, we can use the heuristic selector control policy based on PIDs discussed in Section 3.3 and shown in Figure 1.

To simulate the optimal charging protocol we consider the following parameters for the battery model

$$\begin{cases} R_0 = 1 \text{ (m}\Omega\text{)}, R_1 = 1.5 \text{ (m}\Omega\text{)}, R_2 = 1 \text{ (m}\Omega\text{)} \\ C_1 = 2000 \text{ (kF)}, C_2 = 500 \text{ (kF)}, Q = 50 \text{ (Ah)} \\ \beta = 0.1, u_{\max} = 100 \text{ (A)}, y_{\max} = 0.2 \text{ (V)} \end{cases}$$

The sampling time limits (37) and (38) are given by  $t_s^{(1)} = 500$  (s) and  $t_s^{(2)} = 327.27$  (s), respectively, which are well above the chosen sampling time  $t_s = 0.05$  (s). The resulting bang-ride charging current in (39) and the charging current  $u$  of the heuristic selector control scheme (27) are shown in Figure 3a, as dashed and solid plots respectively. In Figure 3b, the over-potential voltages of the cell are also compared for these two charging profiles. The selector control scheme relies on the measured outputs and PID controllers, whereas the bang-ride charging current (26) is based on the exact battery model and requires accessing the state. Nevertheless, the two charging profiles have almost indistinguishable performances in this experiment, as seen in Figure 3. The



(c) Active constraint tracking errors over time.

Fig. 3. Implementation of the optimal charging profile of the constrained fast charging problem considered in Section 4.2 under two different strategies. The active constraint in the bang-ride profile changes once in this experiment: In the beginning, the current constraint ( $u_t = u_{\max}$ ) is active to charge with the maximum current until  $t = 421.3$  when the voltage constraint becomes active. This constraint remains active until the end of the experiment.

main deviation from the optimal solution happens when the active constraint is switched from current to voltage.

In this experiment, we have used the design technique from [20] to find the PID gains

$$k_1^p = 1, k_1^i = k_1^w = 4, k_1^d = 0.5 \quad (40)$$

This set of gains was compared with the gains

$$k_1^p = 43.23, k_1^i = k_1^w = 0.366, k_1^d = 0 \quad (41)$$

suggested by MATLAB's built-in tuner. Figure (3c) shows the errors that occur after constraint switching under the two different controller tunings. We observe that the gains (40) result in a significantly smaller constraint violation. Whether or not there is a combination of PID gains and anti-windup procedures that guarantees feasibility at all times is not known in general.

## 5 CONCLUSIONS

This paper considered monotone optimal control problems governed by monotone costs, constraints, and dynamics. Such problems appear in many applications, including in the design of fast-charging protocols used for lithium-ion batteries. Optimality conditions were obtained for several classes of monotone optimal control problems, and families of systems that admit bang-ride optimal solutions were identified. It was shown that the corresponding optimal control policies can be implemented by a selector control strategy that switches between a finite number of state feedback laws. These structural results motivate the use of selector strategies based on PID controllers that are typically designed without perfect models and full-state measurements. Simulations of single particle models and equivalent circuit models of lithium-ion batteries in fast-charging problems demonstrated the efficacy of both optimal and heuristic selector control strategies.

## References

- [1] Malin Andersson et al. “Informative battery charging: integrating fast charging and optimal experiments”. In: *IFAC-PapersOnLine* 56.2 (2023), pp. 11160–11166.
- [2] David Angeli and Eduardo D Sontag. “Monotone control systems”. In: *IEEE Transactions on Automatic Control* 48.10 (2003), pp. 1684–1698.
- [3] Karl Johan Åström and Tore Hägglund. *Advanced PID control*. ISA-The Instrumentation, Systems and Automation Society, 2006.
- [4] Josefin Berner et al. “An experimental comparison of PID autotuners”. In: *Control Engineering Practice* 73 (2018), pp. 124–133.
- [5] Cuili Chen, Zhongbao Wei, and Alois Christian Knoll. “Charging optimization for Li-ion battery in electric vehicles: A review”. In: *IEEE Transactions on Transportation Electrification* 8.3 (2021), pp. 3068–3089.
- [6] Ross Drummond et al. “Constrained optimal control of monotone systems with applications to battery fast-charging”. In: *arXiv preprint arXiv:2301.07461* (2023).
- [7] MM Kabir and Dervis Emre Demirocak. “Degradation mechanisms in Li-ion batteries: A state-of-the-art review”. In: *International Journal of Energy Research* 41.14 (2017), pp. 1963–1986.
- [8] Tadeusz Kaczorek. *Positive 1D and 2D systems*. Springer Science & Business Media, 2012.
- [9] Tadeusz Kaczorek. “Positivity and stability of discrete-time nonlinear systems”. In: *Proceedings of the 2nd International Conference on Cybernetics (CYBCONF)*. IEEE. 2015, pp. 156–159.
- [10] Reinhardt Klein et al. “Optimal charging strategies in lithium-ion battery”. In: *Proceedings of the 2011 American Control Conference*. IEEE. 2011, pp. 382–387.
- [11] Dinesh Krishnamoorthy and Sigurd Skogestad. “Systematic design of active constraint switching using selectors”. In: *Computers & chemical engineering* 143 (2020), p. 107106.
- [12] Yang Li et al. “Electrochemical model-based fast charging: Physical constraint-triggered PI control”. In: *IEEE Transactions on Energy Conversion* 36.4 (2021), pp. 3208–3220.
- [13] Bor Yann Liaw et al. “Modeling of lithium ion cells—A simple equivalent-circuit model approach”. In: *Solid state ionics* 175.1-4 (2004), pp. 835–839.
- [14] Saehong Park et al. “Optimal control of battery fast charging based-on Pontryagin’s minimum principle”. In: *Proceedings of the 59th IEEE Conference on Decision and Control (CDC)*. IEEE. 2020, pp. 3506–3513.
- [15] Saehong Park et al. “Optimal experimental design for parameterization of an electrochemical lithium-ion battery model”. In: *Journal of The Electrochemical Society* 165.7 (2018), A1309.
- [16] Anders Rantzer. “Scalable control of positive systems”. In: *European Journal of Control* 24 (2015), pp. 72–80.
- [17] VC Reis et al. “Control of level systems by arduino via PC platform”. In: *Proceedings of the 20th International Conference on System Theory, Control and Computing (ICSTCC)*. IEEE. 2016, pp. 251–256.
- [18] Andrew P Sabelhaus et al. “Safe Supervisory Control of Soft Robot Actuators”. In: *arXiv preprint arXiv:2208.01547* (2022).
- [19] Sadra Sadraddini and Calin Belta. “Safety control of monotone systems with bounded uncertainties”. In: *Proceedings of the 55th Conference on Decision and Control (CDC)*. IEEE. 2016, pp. 4874–4879.
- [20] Hamed Taghavian, Mikael Johansson, and Mohammad Saleh Tavazoei. “Discrete-time SISO LTI Systems with Monotonic Closed-loop Step Responses: Analysis and Control Based on Impulse Response Models”. In: *IFAC-PapersOnLine* 54.9 (2021), pp. 476–481.
- [21] Bing Yu et al. “A novel control scheme for aircraft engine based on sliding mode control with acceleration/deceleration limiter”. In: *IEEE Access* 7 (2018), pp. 3572–3580.